Cellular Oncology (2026) 49:67
https://doi.org/10.1007/s13402-026-01189-3

RESEARCH

A CREM-ITGA2B-MAPK axis drives proliferation and invasiveness in gastric cancer: insights from single-cell analysis

Hongmei Wu[1] · Mengnan Ye[1] · Lisheng Zheng[1] · Yaoyao Zhang[2] · Yan Mei[1] · Yi Lu[3] · Bing Li[3] · Wei Xue[3] · Di Peng[3] · Feiyan Feng[1] · Yue Qiu[1] · Jingbo Sun[4] · Xuegang Sun[5] · Xiuwu Bian[6] · Qingling Zhang[1]

Received: 19 August 2025 / Accepted: 7 March 2026

Abstract

Background Gastric cancer (GC) characterized by profound cellular heterogeneity, with the diversity and interactions of cells within the tumor microenvironment (TME) playing critical roles in tumorigenesis, metastasis, and therapeutic response. However, the underlying mechanisms remain poorly understood. We aimed to elucidate the mechanisms of tumor progression and identify potential therapeutic targets by investigating cellular diversity and communication within the malignant epithelia and tumor microenvironment (TME) in GC.

Methods In-depth single-cell RNA sequencing (scRNA-seq) analyses were performed on 19 fresh samples from 12 GC patients, encompassing primary tumors, lymph nodes, and omental metastases. Subsequent bioinformatics analyses were conducted to characterize cellular heterogeneity, followed by experimental and clinical sample verifications to elucidate the molecular underpinnings of GC progression.

Results Our study identified the cAMP response element modulator (CREM) as a key molecular driver for GC progression, which significant upregulation in malignant epithelial cells. CREM activation promotes aggressive tumor phenotypes and correlates with poorer patient outcomes by regulating the *ITGA2B* promoter and MAPK signaling pathway. Furthermore, we uncovered distinct heterogeneity in T cells and cancer-associated fibroblasts (CAFs) within the GC TME, revealing spatial disparities in immune microenvironments and cell-cell communication across tumor locations.

Conclusion By providing a comprehensive single-cell transcriptomic atlas of GC, this study highlights the pivotal role of CREM in GC progression. These findings deepen our understanding of GC pathogenesis and highlighted the key role of *CREM* in GC progression and advanced our understanding of GC pathogenesis and offer a foundation for developing targeted, personalized therapeutic strategies.

Keywords Gastric cancer · Tumor heterogeneity · scRNA-seq · CREM · ITGA2B · TME

Hongmei Wu, Mengnan Ye, Lisheng Zheng, and Yaoyao Zhang have contributed equally to this work.

✉ Xuegang Sun
sxg_smu@126.com

✉ Xiuwu Bian
bianxiuwu@263.net

✉ Qingling Zhang
zhangqingling@gdph.org.cn

[1] Department of Pathology, Guangdong Provincial People's Hospital, Guangdong Academy of Medical Sciences, Southern Medical University, Guangzhou, China

[2] Department of Obstetrics and Gynecology, Key Laboratory of Birth Defects and Related Diseases of Women and Children of MOE, West China Second University Hospital, Sichuan University, Chengdu, China

[3] Burning Rock Biotech, Guangzhou, China

[4] Department of General Surgery, The Third Affiliated Hospital of Southern Medical University, Guangzhou, China

[5] The Key Laboratory of Molecular Biology, State Administration of Traditional Chinese Medicine, School of Traditional Chinese Medicine, Southern Medical University, Guangzhou, China

[6] Institute of Pathology and Southwest Cancer Center, Southwest Hospital, Third Military Medical University (Army Medical University), Chongqing, China

Published online: 07 April 2026

Abbreviation

NAG	Non-atrophic gastritis
PT	Primary tumo
LN	Lymph node metastasis
OM	Omentum metastasis
DEGs	Differential expression genes
UMAP	Uniform manifold approximation and projection
PT_M	Primary tumor_ malignant cell
PT_N	Primary tumor_ normal cell
CD8+ Tn	CD8+ Naive T cells
CD8+ Temra	CD8+ recently activated effector memory T cells
CD8+ Trm-Tgd	CD8+ tissue-resident memory T (Trm) gamma delta cells
CD4+ Tn	CD4+ Naive T cells
CD8+ Tex	CD8+ exhausted T cells
CD4+ Tcm	CD4+ central memory T cells
CD4+ Treg	CD4+ Regulatory T cells
iCAFs	Inflammatory cancer-associated fibroblasts
apCAFs	Antigen-presenting cancer-associated fibroblasts
mCAFs	Myo-cancer-associated fibroblasts
EBV	Epstein-Barr virus

1 Introduction

Gastric cancer (GC) ranks as the fifth most prevalent malignancy with the fifth leading cause of cancer-related mortality globally [1], and the third leading cancer death (260,400 in 2022) in China [2, 3]. Although the treatment of GC has advanced from simple surgery to a combination of surgery, radiochemotherapy, and immune checkpoint blockade, the efficacy of GC treatment remains suboptimal [4–6], the overall five-year survival rate for GC patients in the United States is merely 36%, with only 7% for late-stage patients experiencing distant metastasis in 2022 [7]. Therefore, identifying novel biomarkers, as well as understanding the mechanisms that regulate the proliferation and metastasis of gastric cancer cells, are crucial for facilitating the development of innovative treatment approaches.

Transcription factors (TFs) are crucial in cell signaling and gene regulation during tumor development. By influencing essential biological processes such as cell proliferation, invasion, and metastasis, aberrant expression of specific TFs is linked to tumor aggressiveness and poor patient prognosis in GC patients [8]. One of the key mechanisms by which TFs contribute to gastric cancer progression is through the promotion of epithelial-mesenchymal transition (EMT), a process that enables tumor cells to acquire migratory and invasive capabilities [9, 10]. Other significant TFs such as YY1 and MAPK1 also play vital roles in the regulation of genes associated with cell cycle dynamics and tumorigenesis [11–13], underscoring the multifaceted impact of TFs in gastric cancer biology. The prognostic potential of these transcription factors is increasingly recognized, as their expression profiles have been utilized to develop predictive models for patient outcomes.

Recent advancements in single-cell RNA sequencing (scRNA-seq) technologies have significantly enhanced the identification of diverse cellular populations and phenotypic states within tumors. This granular perspective facilitates the discovery of rare cell types and unique transcriptomic signatures, which are crucial for understanding tumor dynamics and progression. By identifying distinct cellular states and transcription factors that drive malignant behaviors, scRNA-seq has unveiled molecular signatures linked to tumor aggressiveness, resistance to therapies, and patient prognosis [14]. For example, studies utilizing scRNA-seq have uncovered subtype-specific regulatory networks in various cancers, highlighting the complexity of tumorigenesis and the potential for targeted therapeutic strategies [14, 15].

In this study, we utilized scRNA-seq to dissect regulators driving tumor progression and metastasis in malignant epithelial cells in GC, we find the overexpression of the *CREM* as a key transcriptional regulator associated with tumor progression and poor prognosis, which activates the MAPK signaling pathway via *ITGA2B*, thereby enhancing the malignant characteristics of cancer cells, including their proliferation, migration, and invasiveness. These findings not only expand our comprehension of the intricate cellular interactions in GC but also identify CREM as a potential target for precision medicine.

2 Materials and methods

The detailed materials and methods can be found in the supplemental materials.

3 Results

3.1 A single-cell RNA-seq atlas reveals the cellular heterogeneity across GC primary tissues, lymph nodes, and omental metastasis

Our scRNA-seq analysis examined 19 fresh samples collected from 12 GC patients, including 11 primary tumors (PT), 7 paired lymph nodes (LN) among which 4 exhibited metastasis (Table S1, Fig. 1A), and 1 omental metastasis

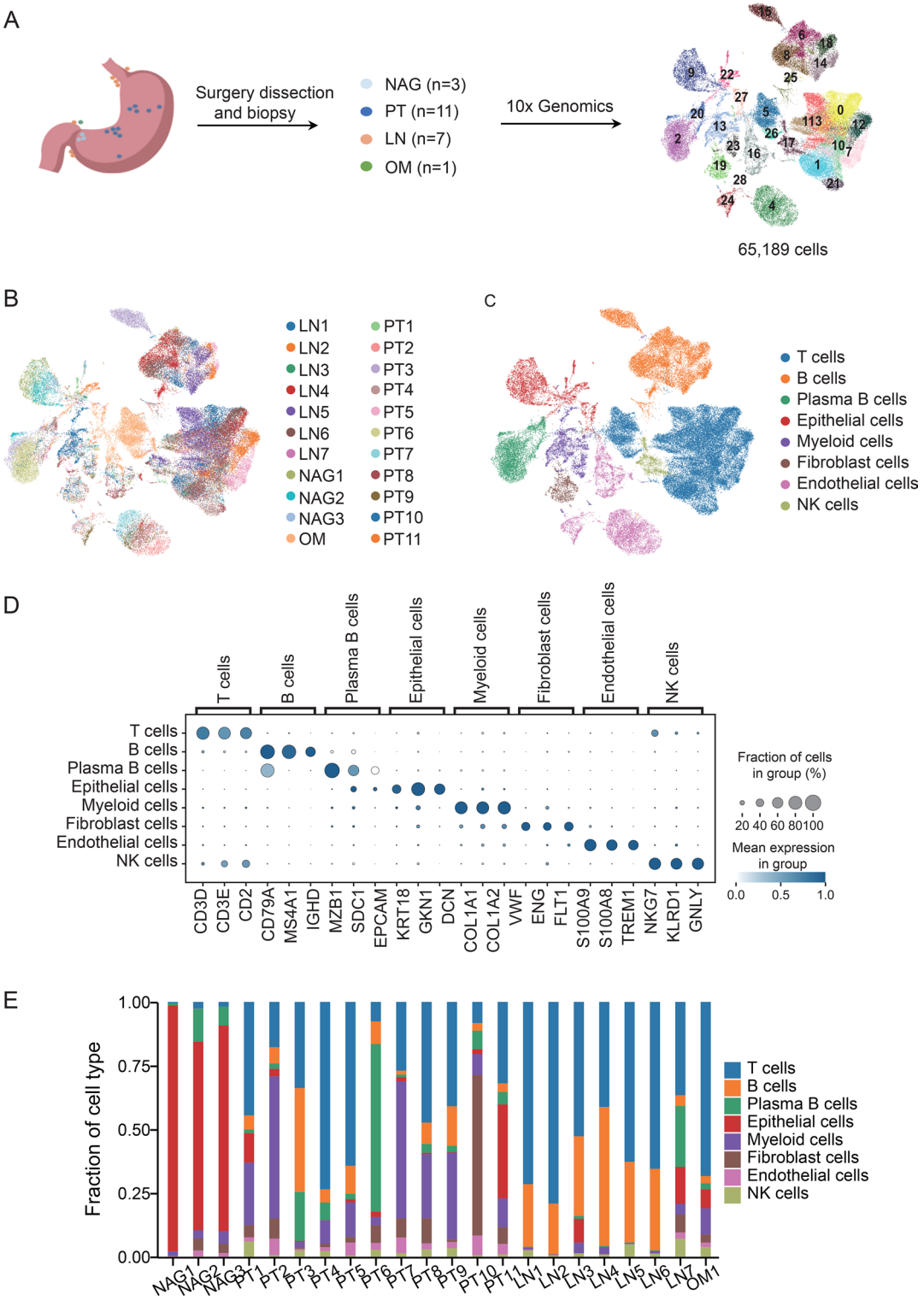

Fig. 1 Single-cell RNA sequencing of gastric primary tumors (PT), lymph nodes (LN), omentum metastasis (OM), and non-atrophic gastritis (NAG). (**A**) A total of 22 samples comprising NAG ($n=3$), PT ($n=11$), LN ($n=7$), and OM ($n=1$) yielded 65,189 cells through 10X Genomic sequencing. (**B**) UMAP plot of all integrated cells, color-coded by sample sources: PT, LN, OM, and NAG. (**C**) The UMAP plot shows the cells, color-coded according to their assigned 8 major cell types. (**D**) A bubble plot representing the expression levels of marker genes characteristic of each cell type. (**E**) The compositional breakdown of the major cell types across the samples

(OM). A public cohort containing 3 non-atrophic gastritis (NAG) samples was included as controls [16]. Following rigorous quality control, we profiled the transcriptomes from 65,189 cells across these samples (Fig. 1A). Among these cells, 47.83%, 37.95%, and 8.88% originated from PT, LN, and OM, respectively. Using Scanpy for dimensionality reduction and unsupervised clustering, we mitigated batch effects across these samples and identified 28 subpopulations (Fig. 1A–B). Utilizing cell-specific markers and the CellTypist tool, these cells were classified into eight cell types: lymphocytes (T, B, and NK cells), plasma cells, epithelial cells, stromal cells (fibroblasts and endothelial cells), and myeloid cells (Table S2, Fig. 1C–D). Notably, B and T cells demonstrated high heterogeneity relative to the other six cell types, implicating their intricate functional landscape (Figs. 1A and 1C). Compared to NAG, PT samples exhibited a significant increase in the proportion of T cells, B cells, plasma cells, myeloid cells, and fibroblasts, suggesting potential modulation by tumor cells (Fig. 1E and Figure S1A).

Cellular composition analysis between PT and LN samples revealed significant enrichment of fibroblasts ($p=0.005$), myeloid cells ($p=0.0043$), endothelial cells ($p=0.056$), and plasma cells ($p=0.0043$) in PT samples, with the enrichment of T cells ($p=0.13$) and B cells ($p=0.0022$) in LN (Figure S1A-B), indicating an immunosuppressive TME in PT samples. The immunocyte composition in PT samples showed high heterogeneity compared to LN samples (Fig. 1A), indicating substantial modulation of the TME by factors beyond tissue composition. Assessment of of EBV status and tumor staging within PT samples revealed a significant increase in T cells ($p=0.012$) in EBV^+ PT samples and a higher prevalence of epithelial cells ($p=0.13$) in EBV^- PT samples, whereas tumor stage did not markedly alter TME composition (Figure S1C-F). These findings highlight the pivotal influence of EBV on T cell enrichment in the TME, independent of tumor progression.

3.2 Distinct transcriptional programs of malignant epithelial cell subpopulations in GC

To distinguish malignant from non-malignant epithelial cells, we employed a comprehensive multi-step approach (for details, see the Methods section), ultimately identifying 1825 malignant and 2423 non-malignant epithelial cells (Fig. 2A). Malignant epithelial cells further classified into seven distinct subpopulations (Fig. 2B). Differential expression analysis identified signature genes for each subpopulation (Figure S2A). Next, we examined the distribution of major subpopulations across different disease locations (Fig. 2C). Notably, C0_TFF1 and C4_PCSK1N were predominantly enriched in NAG, with C4_PCSK1N also present in small numbers in PT samples. C1_S100A4 was shared across all locations, while C2_RPL7A was primarily distributed in PT and LN. In contrast, C5_COL3A1 was specifically enriched in OM. To uncover intrinsic transcriptional programs within different malignant epithelial cell populations, we performed non-negative matrix factorization (NMF), revealing seven distinct transcriptional programs (Fig. 2D) and their associations with malignant subpopulations. Notably, C1_S100A4 and C2_RPL7A were both associated with the NMF5 transcriptional program. Gene set enrichment analysis (GSEA) revealed that NMF5 was significantly enriched in apoptosis, interferon-alpha response, and early estrogen response. KEGG pathway analysis further highlighted its involvement in glutathione metabolism (Fig. 2E). In contrast, C5_COL3A1, which was uniquely present in OM, was primarily associated with NMF2. This transcriptional program was significantly enriched in epithelial-mesenchymal transition (EMT), interferon-alpha and gamma responses, and Notch signaling, suggesting a potential role in tumor invasiveness and immune regulation (Fig. 2F). KEGG pathway analysis further indicated enrichment in focal adhesion and PI3K-Akt signaling pathways. Additionally, in NAG, the predominant C0_TFF1 subpopulation exhibited NMF1 and NMF4 transcriptional programs. Gene enrichment analysis revealed that both programs were strongly associated with TNF-alpha signaling via NF-κB (Figure S2B-C). Another NAG-associated subpopulation, C4_PCSK1N, was associated with the NMF3 transcriptional program, which was enriched in the MAPK signaling pathway and gastric acid secretion (Figure S2D).

Collectively, these findings indicate that malignant epithelial cells in different disease locations exhibit distinct transcriptional programs that regulate key biological functions, influencing their survival, invasiveness, and immune evasion. To further characterize these functional properties, we calculated stemness, proliferation, cell cycle, and EMT scores for malignant cells. Consistent with our previous observations, the C5_COL3A1 subpopulation in OM exhibited a significantly high EMT score (Fig. 2G), whereas other subpopulations had lower EMT scores compared to C5_COL3A1, reinforcing its potential metastatic capability (Fig. 2H). No significant differences were observed across subpopulations for other functional scores (Figure S2E-G).

3.3 CREM as a key transcriptional regulator associated with tumor progression and poor prognosis

To identify key regulators driving tumor progression and metastasis in malignant epithelial cells, we used SCENIC to perform single-cell regulon analysis. By classifying PT epithelial cells into malignant (PT-M) and non-malignant

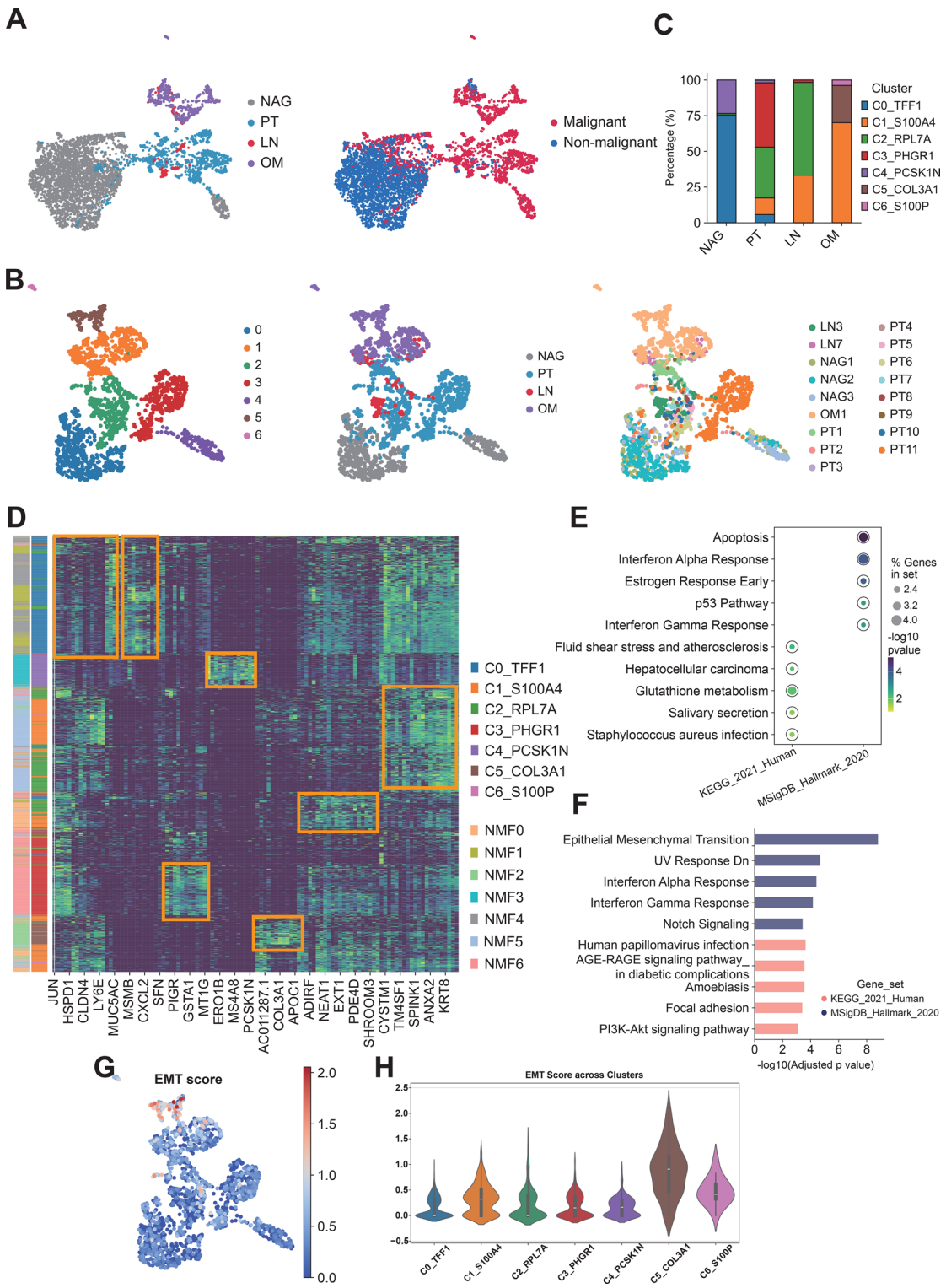

Fig. 2 Subtyping of malignant cells and transcriptional program analysis. (**A**) UMAP plots of epithelial cells, displaying tissue origins and classification into malignant or non-malignant cells. (**B**) Clustering of malignant cells into distinct subpopulations, with the left, middle, and right panels showing clusters, tissue origins, and patient sources, respectively. (**C**) Proportional distribution of seven malignant cell subpopulations across different tissues, with each subpopulation represented by a distinct color. (**D**) Non-negative matrix factorization (NMF) analysis identifying distinct transcriptional programs in malignant cells. The x-axis represents core genes within each transcriptional program, and the y-axis represents cells. The annotation bars on the y-axis indicate cell subpopulation classifications and NMF components. Orange boxes highlight distinct transcriptional programs. (**E-F**) Gene set enrichment analysis (GSEA) of NMF5 (**E**) and NMF2 (**F**) based on KEGG and Hallmark gene sets. (**G**) UMAP plot illustrating the epithelial-mesenchymal transition (EMT) score in malignant cells. (**H**) Distribution of EMT scores among different malignant cell subpopulations

(PT-N) groups and comparing them with NAG, LN, and OM samples, we identified a distinct CREM regulon specificity in PT samples, particularly in PT-M, suggesting CREM may be associated with GC progression (Fig. 3A). However, CREM expression and function in GC cells had not been reported. To elucidate the role of CREM in gastric cancer, we first examined its expression patterns using immunohistochemical (IHC) staining in tumor and adjacent normal tissues (Fig. 3B). Analysis of IHC images from an internal cohort comprising 63 tumor and 43 adjacent normal tissue samples revealed significantly higher CREM expression in tumor tissues (Fig. 3C). Consistently, data from TCGA-STAD [17] and GSE29272 [18] cohorts confirmed higher CREM expression in tumor tissues (Fig. 3D). To further assess the clinical relevance of CREM, Kaplan-Meier survival analysis in an internal patient cohort showed that upregulation of CREM was significantly associated with poorer overall survival (Fig. 3E). Similarly, in the TCGA-STAD cohort, multivariate Cox regression analysis adjusting for tumor stage, age, and gender revealed that higher CREM expression was significantly associated with worse survival outcomes (HR: 1.5, $p=0.033$, Fig. 3F). This association was further validated in two independent cohorts (GSE15460, GSE62254) [19, 20], where higher CREM expression was consistently associated with shorter overall survival (Fig. 3G). To further investigate the biological implications of CREM upregulation in gastric cancer, we performed differential expression analysis by stratifying TCGA-STAD samples into high- and low-CREM expression groups based on the median expression level. Pathway enrichment analysis revealed that the high-CREM group was significantly enriched in cell adhesion, extracellular matrix (ECM)-receptor interactions, PI3K-Akt signaling, and MAPK signaling pathways (Fig. 3H), suggesting a potential role of CREM in intracellular signaling regulation and tumor progression. GSEA analysis revealed significant enrichment of EMT, inflammatory response, and angiogenesis in the high-CREM group (Fig. 3I), highlighting CREM's involvement in tumor invasiveness. Consistently, EMT signature scoring across four independent gene sets confirmed significantly higher EMT activity in CREM-high tumors (Fig. 3J).

Fig. 3 Identification of the tumor-promoting and prognostic value of CREM. (**A**) Heatmap displaying transcription factors' activity in epithelial cells across different tissues. (**B**) Representative images of immunohistochemistry (IHC) staining for CREM in tumor and adjacent normal tissues. (**C**) Statistical analysis of immunohistochemical staining for CREM in tumor and adjacent normal tissues. (**D**) Comparison of CREM expression between tumor and non-tumor tissues in the TCGA-STAD (left) and GSE29272 (right) cohorts. (**E**) Kaplan-Meier survival curves comparing overall survival between high and low CREM expression groups in the internal cohort. (**F**) Multivariate Cox regression analysis incorporating CREM expression and other clinical factors in the TCGA-STAD cohort. * and ** indicate $p<0.05$ and $p<0.01$, respectively. (**G**) Kaplan-Meier survival analysis of CREM expression in GSE15460 (left) and GSE62254 (right) cohorts. (**H**) Pathway enrichment analysis comparing high vs. low CREM expression groups. (**I**) GSEA analysis of CREM-high vs. CREM-low expression groups. (**J**) Comparison of four different EMT signatures between high and low CREM expression groups

3.4 CREM enhances the proliferation, migration, and invasion of GC

The CREM gene has multiple transcripts, and we detected three major bands in gastric cancer cells, two of which have expected molecular weights of about 37kD and 30kD, and the other band with molecular weights between 50kD and 45kD, which is similar to the results reported in the literature [21] (Fig. 4A). In order to investigate the biological behaviors of CREM in GC cells, we firstly constructed CREM shRNA-expression lentivirus (shCREM) and CREM overexpression plasmid containing neomycin (G418) resistance (CREM). MKN28 and HGC27 cell lines with high endogenous CREM expression were chosen to silence CREM. MGC803 and AGS cell lines with low endogenous CREM expression were chosen to overexpress CREM. Transfection efficiency was confirmed by WB and RT-qPCR (Fig. 4B–C). CCK8, colony formation and transwell assay were used to assess the effects of CREM on GC cell proliferation, migration and invasion. The results showed that CREM silenced cells represented markedly weaker promoting effect on the migration, proliferation and invasion of GC cells compare with the control group (Fig. 4D–F, Figure S3A-C). Overexpression of CREM enhances GC cell proliferation, migration and invasion (Fig. 4D–F, Figure S3A-C). Subsequently, to explore the effects of CREM on tumor growth in vivo, we performed subcutaneous tumor formation in nude mice (Fig. 4G–I, Figure S3D). CREM silenced cells represented markedly weaker promoting effect on subcutaneous tumor formation.

3.5 CREM binds to ITGA2B on −1535bp to −1520bp to regulate the MAPK signaling pathway and promote GC progression

It is known that, by binding to ECM, integrins activate MAPK signaling pathways that enhance tumor proliferation, invasion, and survival [22, 23]. Our further studies confirmed that CREM positively regulated the phosphorylation of the key components of MAPK pathway, p38 and ERK1/2 (Fig. 5A). These data suggested that the interaction of CREM with ECM-receptor network, specifically the MAPK pathway, might play an important role in in GC progression. To identify target genes mediating CREM's effects on the MAPK pathway, we utilized the Gene Transcription Regulation Database (GTRD) and intersected it with DEGs

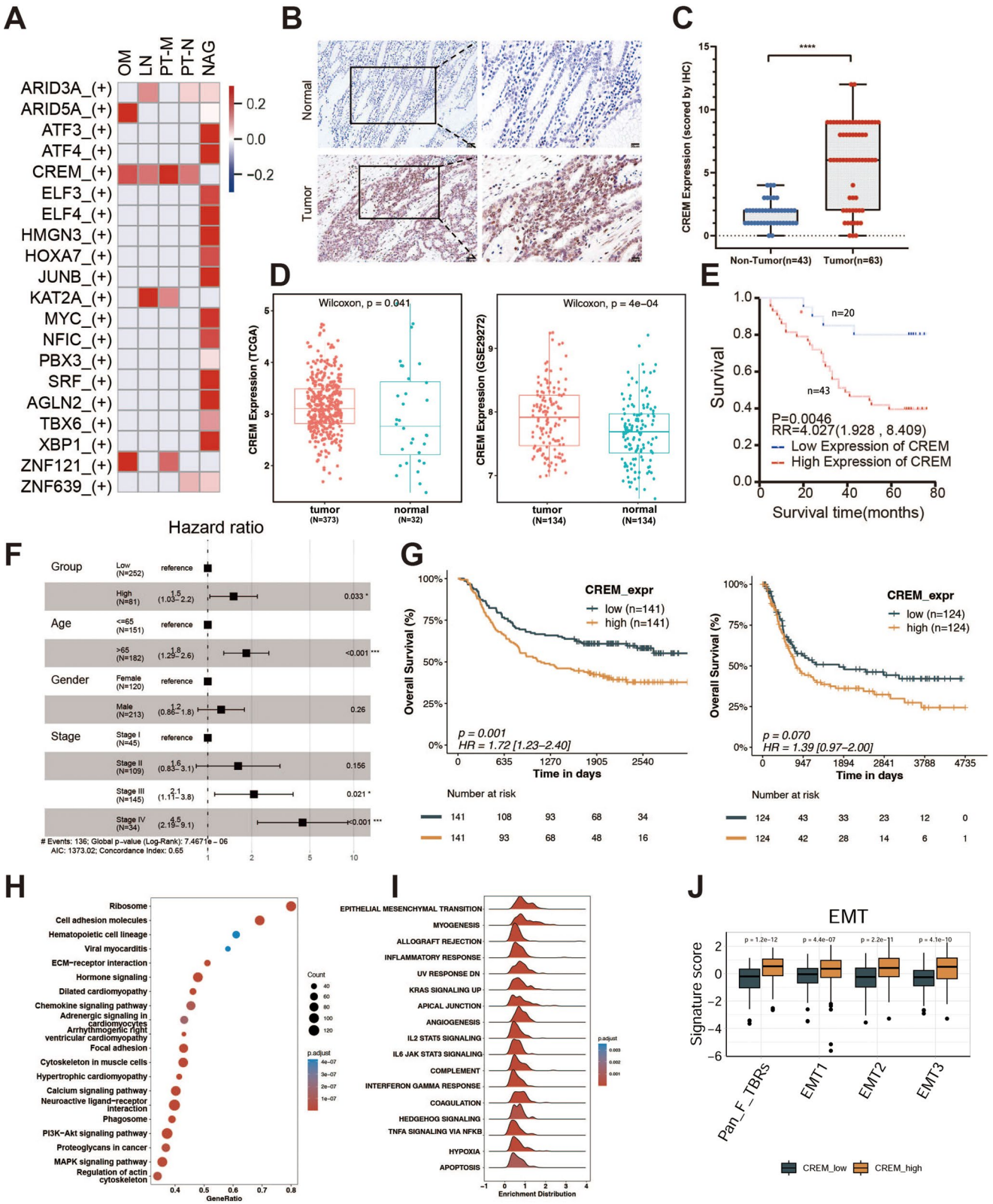

from HGC27-Scram and HGC27-shCREM cells (TableS3) and the integrin gene family profile. This analysis identified ITGA2B as a potential CREM target gene (Figure S4A). CREM positively regulated ITGA2B gene expression at the mRNA and protein levels in GC cell lines (Fig. 5B–C, Figure S4B-C). After confirming the most efficient ITGA2B

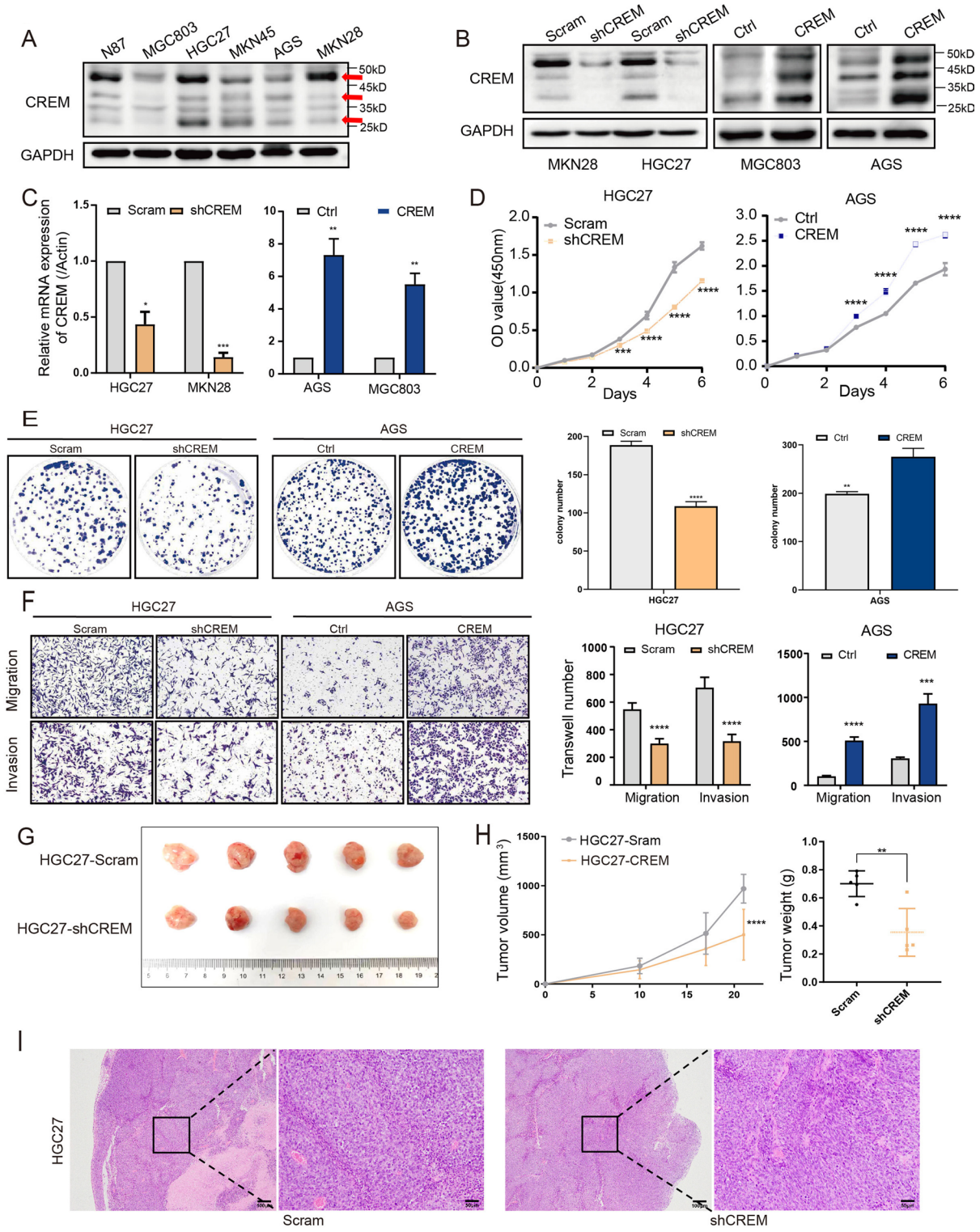

Fig. 4 Investigating the role of CREM in GC tumor cells. (**A**) Western blotting analyzes CREM expression in gastric cancer cell lines. The red arrow indicates the CREM band. (**B-C**) Western blotting and RT-qPCR analyzes the knockdown and overexpression effects of CREM in indicated cell lines. (**D-F**) Effects of knockdown or overexpression of CREM on cell proliferation (**D**), colony formation (**E**), migration and invasion (**F**) in indicated cells. (**G**) Macroscopic observation of the GC subcutaneous tumors in indicated cell lines. (**H**) The volume and the weight analyses for the GC subcutaneous tumors in indicated cell lines. (**I**) H&E staining of the GC Subcutaneous tumors in indicated cell lines. *$p<0.05$, **$p<0.01$, ***$p<0.001$, ****$p<0.0001$

siRNA (three replicates) (Fig. 5D), our rescue experiment verified that CREM overexpression could reverse ITGA2B inhibition (Fig. 5E, S4D) and increased the si-ITGA2B-3-induced p38 and ERK1/2 phosphorylation (Fig. 5F, Figure S4E). Functional cell experiments demonstrated that ITGA2B knockdown significantly reduced cell proliferation (Figure S4F), colony formation (Fig. 5G, Figure S4G), and migration (Fig. 5H, Figure S4H) in both AGS and MGC803 cells, which could be reversed by CREM overexpression (Fig. 5I–J and Figure S4I-J).

These results raised the question of whether CREM regulates ITGA2B by directly binding to it. To address this, we predicted CREM binding sites within the ITGA2B gene promoter using the JASPAR core database and identified six potential binding sites (Fig. 5K). Analysis with the Cistrome DB database further identified critical CREM binding sites at positions −1,901 bp to −1,886 bp (P1) and −1,535 bp to −1,520 bp (P2) upstream of the ITGA2B gene promoter (Figure S4K). Finally, ChIP-qPCR and luciferase reporter assays confirmed that the P2 site (−1535bp to −1520bp) of the ITGA2B promoter directly interacts with CREM (Fig. 5L–M).

To confirm that the observed phenotype was indeed caused by CREM deficiency, a rescue experiment was performed by reintroducing CREM into the deficient cells. The results demonstrated that re-expression of CREM in CREM-knockdown HGC27 cells restored ITGA2B expression and rescued the cell proliferation and migration capabilities (Figure S5A-D). Concurrently, re-expression of ITGA2B in CREM-knockdown HGC27 cells restored tumor growth in nude mice (Figure S5E-G). These results indicate that CREM promotes the proliferation and migration of gastric cancer cells by regulating ITGA2B expression. Next, we investigated whether the upregulation of ITGA2B induced by CREM, which promotes gastric cancer cell proliferation and migration, could be consistently inhibited via the MAPK pathway using an ERK inhibitor (ERKi, SCH772984). The ERK inhibitor downregulated ITGA2B expression in CREM-overexpressing AGS cells and suppressed cell proliferation and migration (Figure S5H-K). In summary, these results indicate that CREM promotes gastric cancer progression by binding to ITGA2B and regulating the MAPK pathway.

3.6 Characteristics of T cells and CAF cells across different tissues

Given that T cells are essential for initiating immune responses that counteract tumorigenesis, we first extracted a total of 15,326 CD8+ and 15,566 CD4+ T cells from the cellular populations and independently categorized them into eight subtypes with unique molecular markers (Fig. 6A–B, Figure S6A-B). Comparative analysis between PT and LN samples revealed a significant enrichment of CD8_IFIT3 ($p=0.05$), CD8_Tex-LAYN ($p=0.0048$), and CD8_Trm-Tgd ($p=0.023$) in PT samples, whereas CD8_Tn-LEF1 cells ($p=0.013$) were more prevalent in LN samples (Fig. 6C). Notably, CD8_Temra-CX3CR1 cells were prominent in OM samples. CD4+ T cell heterogeneity analysis indicated an enrichment of CD4_Tcm-ANXA1 ($p=0.0083$) and CD4_Treg-CTLA4 ($p=0.015$) in PT samples, whereas CD4_Tn-LEF1 cells ($p=0.02$) were more abundant in LN samples (Fig. 6D, Figure S6C). In addition, we further subclassified CAFs, given their critical role in tumor progression and metastasis. CAFs were classified into three discrete subtypes with specific molecular markers (Fig. 6E, Figure S6D), and a significant enrichment of apCAF cells ($p=0.0069$) and iCAF cells ($p=0.023$) was observed in PT samples compared to LN samples, whereas mCAFs showed no significant differences among groups (Fig. 6F).

To further investigate changes in cell communication during gastric cancer progression, we compared the cell-cell interactions between PT and NAG samples using CellChat software. We first observed that a reduction in non-malignant cells' autocrine signaling in PT samples suggests their functionality may be TME-suppressed (Fig. 6G). We further delineated the signaling pathways involved in all interactions by clustering them into four groups based on functional similarities, with the first two groups predominantly present in PT samples (Fig. 6H). Group one included growth factor pathways (e.g., MK, PDGF, IGF, FGF, VEGF), and Group two consisted of pathways associated with cell adhesion and inflammation (e.g., ALCAM, NECTIN, Galectin, Laminin, LIGHT, TNF). The third group involved tumor immunity-related pathways, such as CD46, CD6, CD40, CD226, and TIGIT, present in both NAG and PT samples. In contrast, the fourth group was specific to NAG samples. Interestingly, a majority of the overlapping signaling pathways identified in both PT and NAG samples, including Collagen, MIF, MHC-I, CD46, and THBS, were assigned to distinct groups (Fig. 6I), indicating potential functional disparities across various samples. Subsequent analysis revealed that the Collagen pathway exhibited significant interactions between iCAFs and CD8_Tem-GZMK/neutrophils in PT samples, whereas negligible interactions were observed in NAG samples (Fig. 6J). iCAFs served as essential signal transducers, mediating communication through key ligand-receptor pairs such as COL1A2–CD44 and COL1A1–CD44, facilitating iCAF-immune cell engagement (Figure S6E-F). Similarly, the MIF pathway in PT samples displayed the most pronounced interactions between CD8_Tem-GZMK and CD4_Tem-ANXA1/apCAF/iCAFs, with CD8_Tem-GZMK central to signal transmission (Figure S6G-H). The MIF pathway's

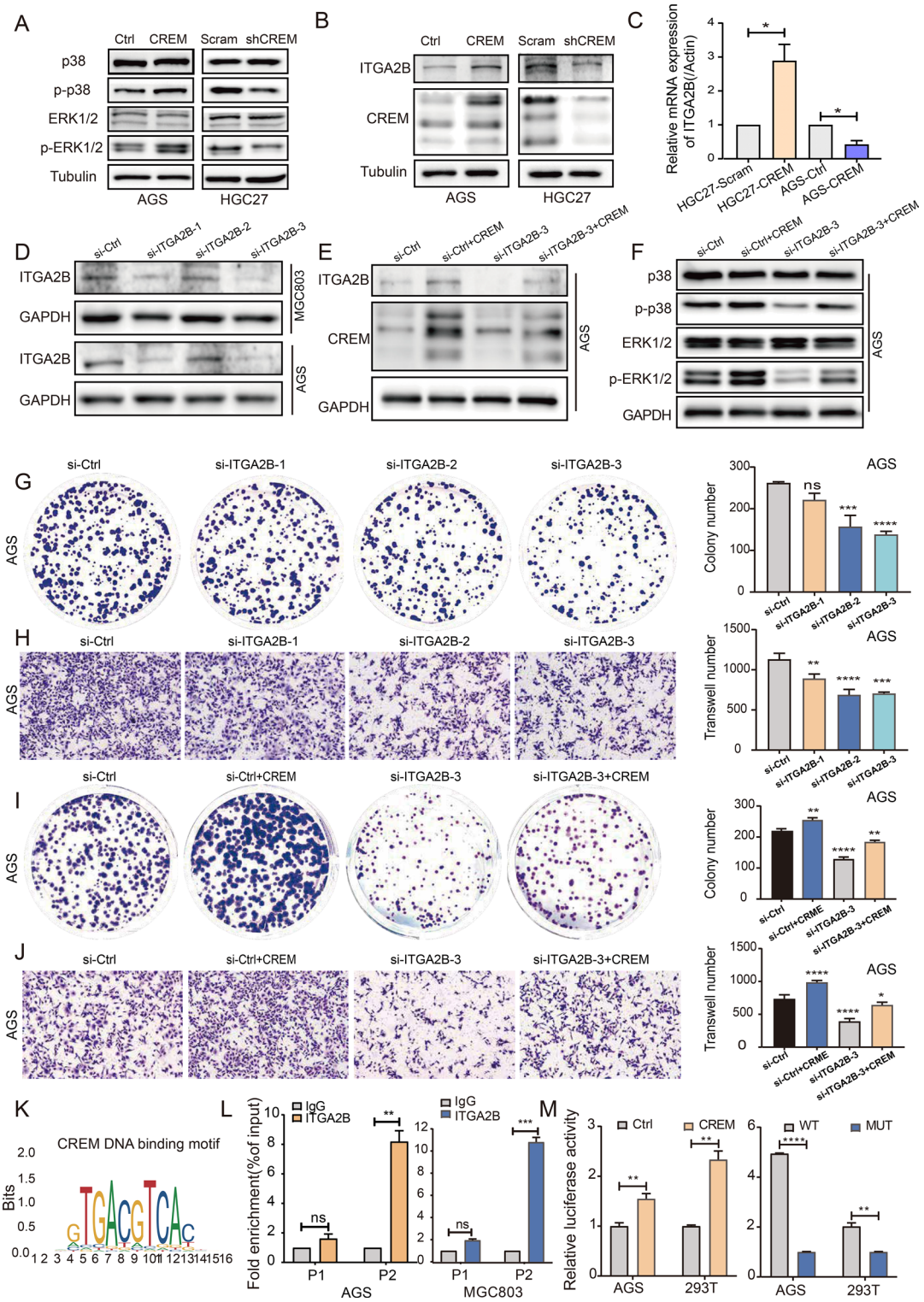

CD74–CD44 and CD74–CXCR4 ligand-receptor pairs were identified as pivotal for signal transduction (Figure S6I).

4 Discussion

GC is one of the most common malignant tumors worldwide, with a relatively high mortality rate [1]. Most gastric cancer patients are diagnosed at an advanced stage, and

Fig. 5 CREM-ITGA2B interaction promotes GC colony formation and cell migration. (**A**) Western blotting analyze effects of overexpression or knockdown of CREM on p38, p-p38, ERK1/2 and p-ERK1/2 in AGC and HGC27 cells. (**B**, **C**) Western blotting(B) and RT-qPCR (**C**) analyze effects of overexpression or knockdown of CREM on ITGA2B gene expression. (**D**) A transfection with three specific siRNA for ITGA2B was performed to select the siRNA with the highest knockdown efficiency in AGC and MGC803 cells. (**E**) Effects of CREM overexpression on ITGA2B expression in AGS cells with siITGA2B were validated by western blot. (**F**) Effects of CREM overexpression on p38, p-p38, ERK1/2 and p-ERK1/2 expression in AGS cells with siITGA2B were validated by western blot. (**G**, **H**) Effects of ITGA2B knockdown on AGS colony formation (**G**) and cell migration (**H**). (**I**, **J**) Colony formation assay(I) and transwell assay (**J**) and were performed in AGS cells with siITGA2B to detect the effect of CREM overexpression on cell migration and colony formation. (**K**) Prediction of conserved CREM recognition sequences in the ITGA2B gene promoter region using the JASPAR database. (**L**) Binding of CREM to the ITGA2B promoter was analyzed by ChIP-seq. (**M**) ITGA2B promoter luciferase activity was determined using a dual-luciferase reporter assay system

conventional chemotherapy has limited efficacy [24]. To further prolong the survival time of patients with GC, identifying novel biomarkers towards GC therapy, and elucidating the mechanisms underlying the progression of GC are extremely important and clinically imperative. This study employed scRNA-seq to meticulously dissect the cellular heterogeneity and communication mechanisms within the GC TME, highlighting the key role of the CREM transcription factor. Previous studies have shown that CREM is an important member of the CREB family, which plays an important role in cell survival, apoptosis and proliferation and can be used as a transcriptional activator or repressor [25, 26]. Through in-depth analysis of single-cell sequencing data, we observed a pronounced increase in CREM regulon activity within the malignant epithelium of primary tumors (PT-M), with a markedly higher expression of CREM in tumor tissues compared to normal tissues. This specificity suggests that CREM is related to GC initiation and progression. Experimental evidence from both in vitro and in vivo models demonstrated that alterations in CREM expression significantly modulate the proliferation, migration, and invasiveness of GC cells, underscoring its critical role in GC progression. Importantly, clinical analyses revealed a robust association between elevated CREM levels and reduced patient survival, along with increased metastasis, highlighting CREM's potential as a prognostic biomarker for GC. These results are consistent with previous study [27]. It is worth noting that low CREM expression in esophageal squamous cell carcinoma enhances the invasion and metastasis of tumor cells and is associated with poor prognosis [28], suggesting its divergent roles across different malignancies. CREM has proved multifaceted roles in T-cell function, contributing to both normal physiology and aberrant responses such as T-cell exhaustion, altered cytokine expression (increased IL-17 and decreased IL-2), and regulatory T-cell suppression [29, 30]. Our exploration of molecular mechanisms has revealed an enrichment of pathways with high CREM expression, notably the MAPK signaling pathway, cell adhesion, and extracellular matrix (ECM) interactions. These findings suggest that CREM may augment the aggressiveness of GC cells by modulating cell adhesion, promoting cell proliferation, and altering cell-microenvironment interactions [31, 32]. Understanding these molecular mechanisms could potentially lead to the development of targeted therapies for GC.

Through predictive and screening analyses of target genes, ITGA2B has been identified as a potential downstream target of CREM. Emerging evidence demonstrates that ITGA2B overexpression in malignant cells promotes tumor progression through extracellular matrix-mediated adhesion, migration, and invasion. Elevated ITGA2B expression correlates with adverse outcomes in breast cancer [33] and clear cell renal cell carcinoma [34]. Our findings confirm that CREM binds directly to the P2 domain of the ITGA2B promoter (−1535 to −1520 bp), thereby upregulating its expression and influencing the MAPK signaling pathway. Futhermore, CREM promotes the proliferation and migration of gastric cancer cells by regulating ITGA2B, which can be inhibited by ERKi. This discovery not only highlights the pivotal role of CREM in the malignancy of GC cells but also elucidates the mechanism by which CREM modulates the MAPK pathway through the regulation of the ITGA2B promoter's P2 domain, thus promoting GC progression. However, the multifaceted roles of CREM as a transcription factor in normal cellular functions beyond cancer progression present challenges for its targeting. Consequently, further research is warranted to refine targeted therapeutic strategies, precisely regulate CREM activity, and assess potential side effects prior to clinical development. This is essential for minimizing off-target effects and ensuring the specificity of cancer cell targeting.

Tumor heterogeneity significantly complicates the diagnosis and treatment of GC scRNA-seq is essential for understanding GC diversity. Despite this, the heterogeneity between PT and LN samples remained undisclosed. This study employed scRNA-seq to deeply analyze cellular distribution within the TME, revealing an increase in T cells, B cells, plasma cells, myeloid cells, and fibroblasts in PT samples compared to NAG samples. This increase may facilitate tumor immune evasion, aligning with previous research [35]. PT samples exhibit pronounced immunosuppression with notable increases in fibroblasts, myeloid, and endothelial cells relative to LN samples. The further analysis revealed that EBV+ PT samples showed a higher T cell density, indicating a stronger immune response to EBV infection, while EBV- PT samples had more epithelial cells,

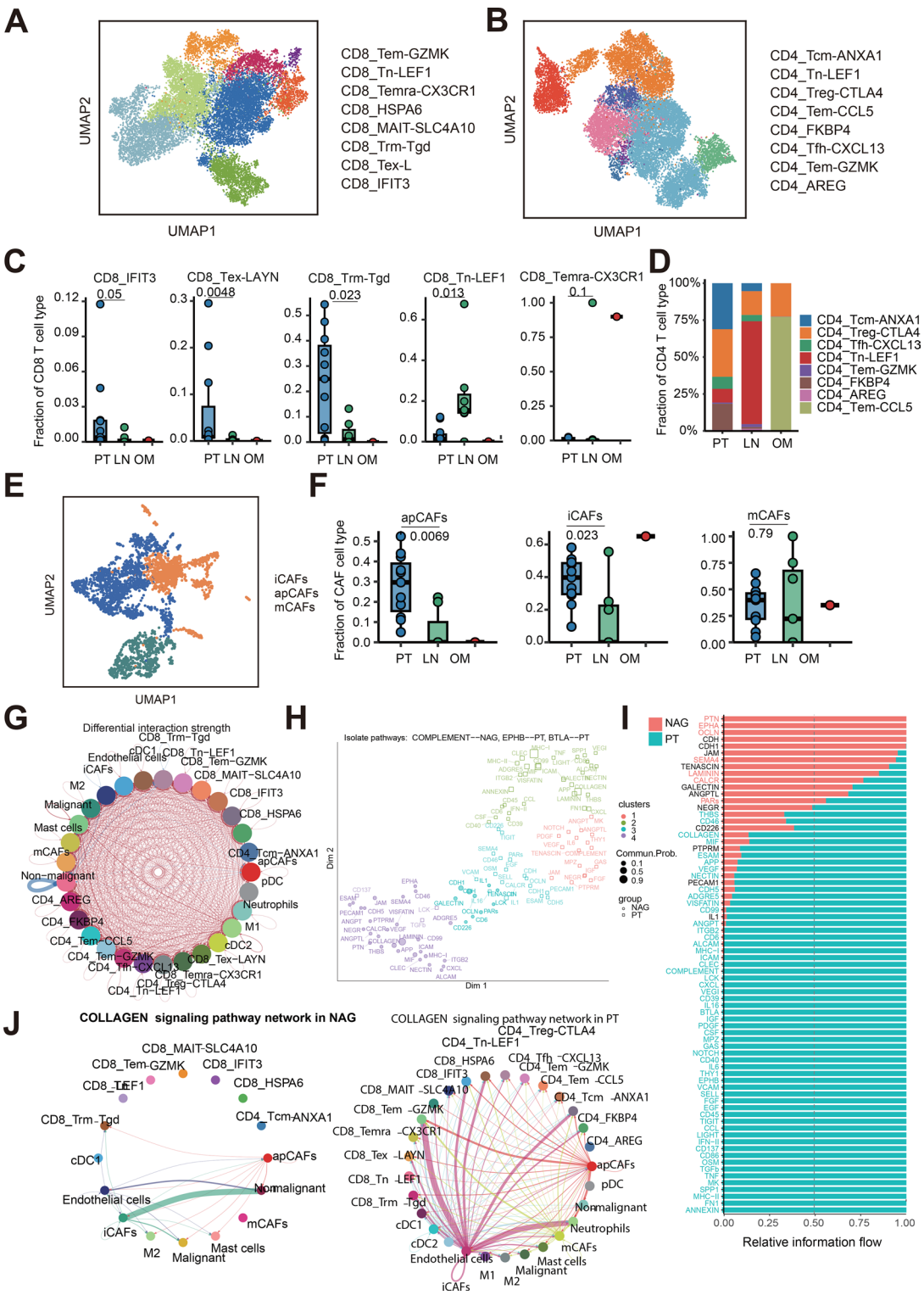

suggesting enhanced immune suppression. Additionally, we identified seven distinct transcriptional programs associated with different malignant subpopulations through NMF analysis. Notably, NMF2 was specifically associated with OM and was significantly enriched in EMT, interferon-alpha and gamma responses, and Notch signaling, suggesting its potential role in tumor invasiveness and immune regulation. Heterogeneity in functional programs, cellular distribution and immune microenvironment of different disease locations enabled us to gain insight into the evolutionary mechanisms of malignant cells in GC and to develop more effective methods for cancer intervention.

Fig. 6 Comparative analysis of T cells and CAFs across different tissues. (**A**) UMAP plot presenting eight distinct CD8+ T cell subtypes. (**B**) UMAP plot presenting eight distinct CD4+ T cell subtypes. (**C**) Box plot showing the differential distribution of CD4+ T cell subpopulations across different tissues. (**D**) Proportional distribution of CD4+ T cell subtypes across different tissues. (**E**) UMAP plot presenting three distinct CAF subtypes. (**F**) Box plot showing the distribution of CAF subtypes across different tissues. (**G**) Circle plots illustrating the differential interaction strength between various cell types in PT and NAG. (**H**) Projection and clustering of signaling pathways from PT and NAG onto a shared two-dimensional manifold, based on functional similarities of inferred networks. Circle and square symbols represent signaling networks from NAG and PT, respectively. Each dot or square represents the communication network of an individual signaling pathway, with size proportional to communication probability. Different colors indicate distinct signaling pathway groups. (**I**) Comparison of overall signaling pathway flow in PT and NAG, ranked by inferred network information flow discrepancies. Pathways enriched in NAG are highlighted in red, while those enriched in PT are indicated in green, representing relative communication probabilities. (**J**) Intercellular communication networks related to the collagen pathway among different cell types in NAG and PT, where line thickness correlates with interaction frequency and strength

Although our experimental data demonstrate that CREM intrinsically drives tumor progression through the ITGA2B-MAPK axis, our single-cell panoramic analysis places these findings within a broader context. We observed that gastric cancer tissues are enriched with immunosuppressive iCAFs and exhausted T cells. This suggests a possibility: the aggressive phenotype (high proliferation and migration) driven by CREM may also remodel the local microenvironment to recruit these stromal components; conversely, this specific immunosuppressive microenvironment may provide the necessary signals to sustain high CREM expression. We acknowledge that our current data are correlative and do not establish whether CREM directly modulates these TME features in vivo. Future studies employing mouse GC cell line such as YTN116 with immunocompetent C57 mice in orthotopic model will help address this important question. By comparing the TME composition—specifically the infiltration and functional status of iCAFs and T cells—in mice tumors upon CREM-overexpression or CREM-knockdown, we can directly test whether CREM actively sculpts the immunosuppressive landscape. Such experiments will be critical to determine if the correlation observed in our patient data represents a functional driver of immune evasion and to fully elucidate the mechanisms by which CREM contributes to poor clinical prognosis.

5 Conclusion

In conclusion, our study synthesizes key findings from single-cell transcriptomic analysis, revealing significant heterogeneity within epithelia and the TME of GC. We identified that the transcription factor CREM enhances cancer cell proliferation and invasion through targeting ITGA2B. These insights deepen our understanding of the molecular mechanisms underlying GC and propose potential therapeutic targets for CREM-directed therapy. Moving forward, further investigation is warranted to translate these findings into tangible clinical applications.

Supplementary Information The online version contains supplementary material available at https://doi.org/10.1007/s13402-026-01189-3.

Author contributions QZ, XB, XS, XB and YZ made substantial contributions to the conception and design of this study. YZ, HW, LZ and YM wrote the manuscript. LZ, MY, HM and YM performed experiments and analyzed data. LZ, YL, BL, WX and DP participated in the design of figures in this study. FF, YQ and JS collected gastric cancer sample. All authors read and approved the final manuscript.

Funding This project was supported by grants of High-level Hospital Construction Project (XWB YKY-KF202204 and QLZ, DFJH-BF202108); Key R&D Program Projects in Guangdong Province (2021B0101420005); National Natural Science Foundation of China (QLZ, 82173033; YWX, 82102712); China Postdoctoral Science Foundation (YWX, 2021M690751); Guangdong Provincial Key Laboratory of Artificial Intelligence in Medical Image Analysis and Application (2022B1212010011).

Data availability All raw and processed data have been deposited in the BIG Data Center (Beijing Institute of Genomics, Chinese Academy of Sciences) under accession number PRJCA018466.

Declarations

Ethics declarations The study has obtained approval from Guangdong Provincial People's Hospital Ethics Committee (ID: 2020-271 H-1). Experiments were performed in accordance with the Declaration of Helsinki.

Competing interests The authors declare no competing interests.

References

1. F. Bray, M. Laversanne, H. Sung, J. Ferlay, R.L. Siegel, I. Soerjomataram, A. Jemal, Global cancer statistics 2022: GLOBOCAN

estimates of incidence and mortality worldwide for 36 cancers in 185 countries. CA. Cancer. J. Clin. **74**, 229–263 (2024)
2. W. Cao, H.D. Chen, Y.W. Yu, N. Li, W.Q. Chen, Changing profiles of cancer burden worldwide and in China: a secondary analysis of the global cancer statistics 2020. Chin. Med. J. (Engl) **134**, 783–791 (2021)
3. B. Han, R. Zheng, H. Zeng, S. Wang, K. Sun, R. Chen, L. Li, W. Wei, J. He, Cancer incidence and mortality in China, 2022. J Natl Cancer Cent. **4**, 47–53 (2024)
4. Y.K. Kang, N. Boku, T. Satoh, M.H. Ryu, Y. Chao, K. Kato, H.C. Chung, J.S. Chen, K. Muro, W.K. Kang, K.H. Yeh, T. Yoshikawa, S.C. Oh, L.Y. Bai, T. Tamura, K.W. Lee, Y. Hamamoto, J.G. Kim, K. Chin, D.Y. Oh, K. Minashi, J.Y. Cho, M. Tsuda, L.T. Chen, Nivolumab in patients with advanced gastric or gastro-oesophageal junction cancer refractory to, or intolerant of, at least two previous chemotherapy regimens (ONO-4538-12, ATTRACTION-2): a randomised, double-blind, placebo-controlled, phase 3 trial. Lancet **390**, 2461–2471 (2017)
5. E.C. Smyth, M. Nilsson, H.I. Grabsch, N.C. van Grieken, F. Lordick, Gastric cancer. Lancet **396**, 635–648 (2020)
6. A.C. Society, Cancer Facts & Figures 2024., Atlanta: American Cancer Society, (2024)
7. A.P. Thrift, H.B. El-Serag, Burden of gastric cancer, Clin Gastroenterol Hepatol. **18**, 534–542 (2020)
8. L. Zhou, Z. Chen, Y. Wu, H. Lu, L. Xin, Prognostic signature composed of transcription factors accurately predicts the prognosis of gastric cancer patients. Cancer Cell. Int. **21**, 357 (2021)
9. C. Huang, R. Chen, F. Zheng, Y. Tang, X. Wang, Z. Chen, X. Lai, Inhibitory role of ATF3 in gastric cancer progression through regulating cell EMT and stemness. Cancer Cell. Int. **21**, 127 (2021)
10. H. Shen, H. Zhu, Y. Chen, Z. Shen, W. Qiu, C. Qian, J. Zhang, ZEB1-induced LINC01559 expedites cell proliferation, migration and EMT process in gastric cancer through recruiting IGF2BP2 to stabilize ZEB1 expression. Cell. Death Dis. **12**, 349 (2021)
11. J. Wang, X. Wu, W. Dai, J. Li, L. Xiang, W. Tang, J. Lin, W. Zhang, G. Liu, Q. Yang, Z. Lin, Y. Sun, Y. Zhang, Y. Chen, G. Li, A. Li, S. Liu, Y. Li, J. Wang, The CCDC43-ADRM1 axis regulated by YY1, promotes proliferation and metastasis of gastric cancer. Cancer Lett. **482**, 90–101 (2020)
12. Y. Wang, Z. Guo, Y. Tian, L. Cong, Y. Zheng, Z. Wu, G. Shan, Y. Xia, Y. Zhu, X. Li, Y. Song, MAPK1 promotes the metastasis and invasion of gastric cancer as a bidirectional transcription factor. BMC Cancer **23**, 959 (2023)
13. W. Yuan, Y. Shi, S. Dai, M. Deng, K. Zhu, Y. Xu, Z. Chen, Z. Xu, T. Zhang, S. Liang, The role of MAPK pathway in gastric cancer: unveiling molecular crosstalk and therapeutic prospects. J. Transl. Med. **22**, 1142 (2024)
14. M. Hong, S. Tao, L. Zhang, L.T. Diao, X. Huang, S. Huang, S.J. Xie, Z.D. Xiao, H. Zhang, RNA sequencing: new technologies and applications in cancer research. J. Hematol. Oncol. **13**, 166 (2020)
15. Y. Yang, Z. Liu, Y. Wei, S. He, A. Gu, Z. Li, J. Li, Z. Xu, B. Cen, Single-cell multi-omics analysis reveals candidate therapeutic drugs and key transcription factor specifically for the mesenchymal subtype of glioblastoma. Cell. Biosci. **14**, 151 (2024)
16. P. Zhang, M. Yang, Y. Zhang, S. Xiao, X. Lai, A. Tan, S. Du, S. Li, Dissecting the single-cell Transcriptome network underlying gastric premalignant lesions and early gastric cancer. Cell. Rep. **27**, 1934–1947e1935 (2019)
17. F.R. Lucchesi, N.D. Aredes, The Cancer Genome Atlas Stomach Adenocarcinoma Collection (TCGA-STAD) (Version 3) (The Cancer Imaging Archive). https://doi.org/10.7937/K9/TCIA.2016.GDHL9KIM
18. G. Wang, N. Hu, H. Yang, L. Wang, H. Su, C. Wang, R. Clifford, E. Dawsey, J. Li, T. Ding, X. Han, C. Giffen, A. Goldstein, P. Taylor, M. Lee, Comparison of global gene expression of gastric cardia and noncardia cancers from a high-risk population in China. PLoS One **8**, e63826 (2013)
19. V. Subhash, M. Yeo, L. Wang, S.T.F. Wong, W.T. Wi. Thuya, P. Peethala, M. Soe, D. Tan, N. Padmanabhan, E. Baloglu, S. Shacham, P. Tan, H. Koeffler, W. Yong, Anti-tumor efficacy of selinexor (KPT-330) in gastric cancer is dependent on nuclear accumulation of p53 tumor suppressor. Sci. Rep. **8**, 12248 (2018)
20. R. Cristescu, J. Lee, M. Nebozhyn, K. Kim, J. Ting, S. Wong, J. Liu, Y. Yue, J. Wang, K. Yu, X. Ye, I. Do, S. Liu, L. Gong, J. Fu, J. Jin, M. Choi, T. Sohn, J. Lee, J. Bae, S. Kim, S. Park, I. Sohn, S. Jung, P. Tan, R. Chen, J. Hardwick, W. Kang, M. Ayers, D. Hongyue, C. Reinhard, A. Loboda, S. Kim, A. Aggarwal, Molecular analysis of gastric cancer identifies subtypes associated with distinct clinical outcomes. Nat Med. **21**, 449–456 (2015)
21. H. Kaprio, V.D. Heuser, K. Orte, M. Tukiainen, I. Leivo, M. Gardberg, Expression of transcription factor CREM in human tissues. J. Histochem. Cytochem. **69**, 495–509 (2021)
22. L.V. Abruzzo, C.D. Herling, G.A. Calin, C. Oakes, L.L. Barron, H.E. Banks, V. Katju, M.J. Keating, K.R. Coombes, Trisomy 12 chronic lymphocytic leukemia expresses a unique set of activated and targetable pathways. Haematologica **103**, 2069–2078 (2018)
23. Y. Zhu, K. Zhao, A. Prinz, K. Keyvani, N. Lambertz, I. Kreitschmann-Andermahr, T. Lei, U. Sure, Loss of endothelial programmed cell death 10 activates glioblastoma cells and promotes tumor growth. Neuro. Oncol. **18**, 538–548 (2016)
24. E.V. Cutsem, X. Sagaert, B. Topal, K. Haustermans, H. Prenen, Gastric cancer. Lancet **388**, 2654–2664 (2016)
25. P.K. Brindle, M.R. Montminy, The CREB family of transcription activators. Curr. Opin. Genet. Dev. **2**, 199–204 (1992)
26. S.P. Persengiev, M.R. Green, The role of ATF/CREB family members in cell growth, survival and apoptosis. Apoptosis **8**, 225–228 (2003)
27. K. Yu, L. Kuang, T. Fu, C. Zhang, Y. Zhou, C. Zhu, Q. Zhang, Z. Zhang, A. Le, CREM is correlated with immune-suppressive microenvironment and predicts poor prognosis in gastric Adenocarcinoma. Front. Cell. Dev. Biol. **9**, 697748 (2021)
28. Y. Wang, S. Zhou, X. Yang, H. Shi, M. Li, Q. Xue, X. Huang, X. Wang, H. Wang, J. Zhang, Low expression of cyclic AMP response element modulator-1 can increase the migration and invasion of esophageal squamous cell carcinoma. Tumour Biol. **34**, 3649–3657 (2013)
29. C.J. Maine, J.R. Teijaro, K. Marquardt, L.A. Sherman, PTPN22 contributes to exhaustion of T lymphocytes during chronic viral infection. Proc Natl Acad Sci U S A. **113**, E7231–E7239 (2016)
30. S.H. Subramanyam, K. Tenbrock, The cAMP responsive element modulator (CREM) is a regulator of CD4(+) T cell function. Biol. Chem. **402**, 1591–1596 (2021)
31. R.A. Saxton, D.M., Sabatini, mTOR signaling in growth, metabolism, and disease. Cell **168**, 960–976 (2017)
32. A. Szwed, E. Kim, E. Jacinto, Regulation and metabolic functions of mTORC1 and mTORC2. Physiol. Rev. **101**, 1371–1426 (2021)
33. J.B. Schaubaecher, B. Smiljanov, F. Haring, K. Steiger, Z. Wu, A. Ugurluoglu, J. Luft, S. Ballke, S. Mahameed, V. Schneewind, J. Hildinger, M. Canis, L.A. Mittmann, C. Braun, G. Zuchtriegel, R. Kaiser, L. Nicolai, M. Mack, W. Weichert, K. Lauber, B. Uhl, C.A. Reichel, Procoagulant platelets promote immune evasion in triple-negative breast cancer. Blood **144**, 216–226 (2024)
34. X. Lu, F. Wan, H. Zhang, G. Shi, D. Ye, ITGA2B and ITGA8 are predictive of prognosis in clear cell renal cell carcinoma patients. Tumour Biol. **37**, 253–262 (2016)
35. V. Kumar, K. Ramnarayanan, R. Sundar, N. Padmanabhan, S. Srivastava, M. Koiwa, T. Yasuda, V. Koh, K.K. Huang, S.T. Tay, S.W.T. Ho, A.L.K. Tan, T. Ishimoto, G. Kim, A. Shabbir, Q. Chen, B. Zhang, S. Xu, K.P. Lam, H.Y.J. Lum, M. Teh, W.P. Yong, J.B.Y. So, P. Tan, Single-cell Atlas of lineage States, tumor

microenvironment, and subtype-specific expression programs in gastric cancer. Cancer Discov. **12**, 670–691 (2022)